Article

Direct Detection of a Hydrogen Ligand in the [NiFe] Center of the Regulatory H-Sensing Hydrogenase from *Ralstonia eutropha* in Its Reduced State by HYSCORE and ENDOR Spectroscopy

Marc Brecht, Maurice van Gastel, Thorsten Buhrke, Brbel Friedrich, and Wolfgang Lubitz

J. Am. Chem. Soc., **2003**, 125 (43), 13075-13083• DOI: 10.1021/ja036624x • Publication Date (Web): 01 October 2003

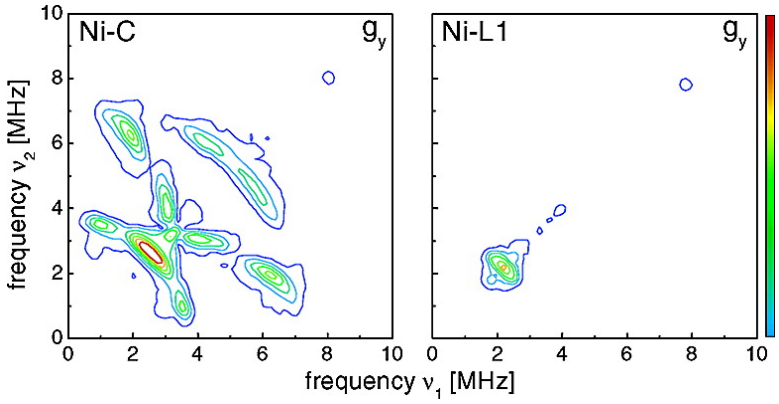

More About This Article

Additional resources and features associated with this article are available within the HTML version:

- Supporting Information
- Links to the 21 articles that cite this article, as of the time of this article download
- Access to high resolution figures
- Links to articles and content related to this article
- Copyright permission to reproduce figures and/or text from this article

View the Full Text HTML

J|A|C|S
ARTICLES
Published on Web 10/01/2003

Direct Detection of a Hydrogen Ligand in the [NiFe] Center of the Regulatory H_2-Sensing Hydrogenase from *Ralstonia eutropha* in Its Reduced State by HYSCORE and ENDOR Spectroscopy

Marc Brecht,[†,||] Maurice van Gastel,[‡] Thorsten Buhrke,[§] Bärbel Friedrich,[§] and Wolfgang Lubitz*[,‡]

Contribution from the Max-Volmer-Laboratorium für Biophysikalische Chemie, Fakultät für Mathematik und Naturwissenschaften, Technische Universität Berlin, D-10623 Berlin, Germany; Max-Planck-Institut für Bioanorganische Chemie, P.O. Box 101365, D-45413 Mülheim an der Ruhr, Germany; and Institut für Biologie, Humboldt-Universität Berlin, D-10115 Berlin, Germany

Received June 11, 2003; E-mail: lubitz@mpi-muelheim.mpg.de

Abstract: The regulatory H_2-sensing [NiFe] hydrogenase of the β-proteobacterium *Ralstonia eutropha* displays an Ni−C "active" state after reduction with H_2 that is very similar to the reduced Ni−C state of standard [NiFe] hydrogenases. Pulse electron nuclear double resonance (ENDOR) and four-pulse ESEEM (hyperfine sublevel correlation, HYSCORE) spectroscopy are applied to obtain structural information on this state via detection of the electron−nuclear hyperfine coupling constants. Two proton hyperfine couplings are determined by analysis of ENDOR spectra recorded over the full magnetic field range of the EPR spectrum. These are associated with nonexchangeable protons and belong to the β-CH_2 protons of a bridging cysteine of the NiFe center. The signals of a third proton exhibit a large anisotropic coupling ($A_x = 18.4$ MHz, $A_y = -10.8$ MHz, $A_z = -18$ MHz). They disappear from the ^{1}H region of the ENDOR spectra after exchange of H_2O with ^2H_2O and activation with $^2H_2$ instead of H_2 gas. They reappear in the ^{2}H region of the ENDOR and HYSCORE spectra. Based on a comparison with the spectroscopically similar [NiFe] hydrogenase of *Desulfovibrio vulgaris* Miyazaki F, for which the *g*-tensor orientation of the Ni−C state with respect to the crystal structure is known (Foerster et al. *J. Am. Chem. Soc.* **2003**, *125*, 83−93), an assignment of the ^{1}H hyperfine couplings is proposed. The exchangeable proton resides in a bridging position between the Ni and Fe and is assigned to a formal hydride ion. After illumination at low temperature ($T = 10$ K), the Ni−L state is formed. For the Ni−L state, the strong hyperfine coupling observed for the exchangeable hydrogen in Ni−C is lost, indicating a cleavage of the metal−hydride bond(s). These experiments give first direct information on the position of hydrogen binding in the active NiFe center of the regulatory hydrogenase. It is proposed that such a binding situation is also present in the active Ni−C state of standard hydrogenases.

Introduction

Molecular hydrogen plays an important role in the metabolism of many microorganisms. Both H_2 production and H_2 uptake are catalyzed by hydrogenases. These oxidoreductases are classified as [NiFe], [Fe]-only, and metal-free hydrogenases according to the composition of their hydrogen-activating sites (for review, see ref 1). Standard [NiFe] hydrogenases are heterodimeric enzymes that harbor the active site in the large subunit and three iron sulfur clusters in the small subunit. Crystal structures of [NiFe] hydrogenases are available for the sulfate-reducing bacteria *Desulfovibrio gigas*[2], *Desulfovibrio vulgaris* Miyazaki F,[3,4] *Desulfovibrio fructosovorans*,[5] and *Desulfovibrio desulfuricans*.[6] They all show a conserved coordination geometry of the active site that is depicted in Figure 1.

The [NiFe] active site is a heterobimetallic center consisting of one nickel and one iron atom. The two metals are bridged by a pair of sulfurs provided by two cysteines, and the nickel atom is ligated by two additional cysteine thiolate groups. Three diatomic ligands, one CO and two CNs, are bound to the iron as shown by FTIR analysis.[7−9] The aerobically isolated enzyme,

[†] Technische Universität Berlin.
[‡] Max-Planck-Institut für Bioanorganische Chemie.
[§] Institut für Biologie.
[||] Present address: Institut für Experimentalphysik, Freie Universität Berlin, Arnimallee 14, D-14195 Berlin, Germany.

(1) Vignais, P. M.; Billoud, B.; Meyer, J. *FEMS Microbiol. Rev.* **2001**, *25*, 455−501.
(2) Volbeda, A.; Charon, M.-V.; Piras, C.; Hatchikian, E. C.; Frey, M.; Fontecilla-Camps, J. C. *Nature* **1995**, *373*, 580−587.
(3) Higuchi, Y.; Yagi, T.; Yasuoka, N. *Structure* **1997**, *5*, 1671−1680.
(4) Higuchi, Y.; Ogata, H.; Miki, K.; Yasuoka, N.; Yagi, T. *Structure* **1999**, *7*, 549−556.
(5) Nicolet, Y.; Piras, C.; Legrand, P.; Hatchikian, C. E.; Fontecilla-Camps, J. C. *Structure* **1999**, *15*, 13−23.
(6) Matias, P. M.; Soares, C. M.; Saraiva, L. M.; Coelho, R.; Morais, J.; Le Gall, J.; Carrondo, M. A. *J. Biol. Inorg. Chem.* **2001**, *6*, 63−81.
(7) Happe, R. P.; Roseboom, W.; Pierik, A. J.; Albracht, S. P. J.; Bagley, K. A. *Nature* **1997**, *385*, 126−126.

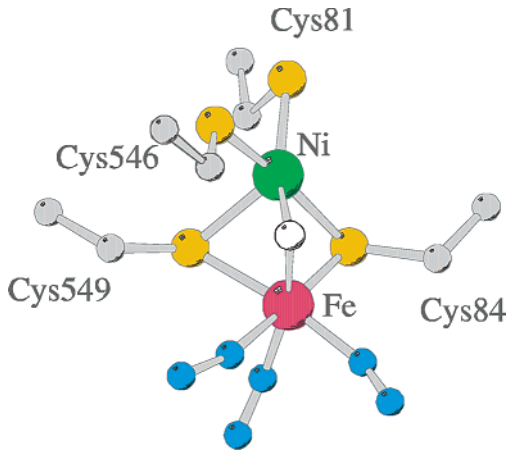

Figure 1. Schematic representation of the active site of [NiFe] hydrogenase based on the crystal structure of *D. vulgaris* Miyazaki F,[3] where the diatomic ligands to iron (either CN, CO, or SO) have been indicated in blue. The bridging ligand (white) was suggested to be an oxygen species for the as-isolated enzyme and a hydride (H^-) for the reduced enzyme.[10,11]

referred to "as-isolated", is predominantly present in the oxidized state and contains an additional bridging ligand, presumably an oxygen species.[10]

At least seven redox states have been assigned to [NiFe] hydrogenases (for a review, see refs 12 and 13). The standard [NiFe] hydrogenase in its oxidized form is inactive and can be activated with hydrogen, a process that correlates with the loss of the oxygen ligand. Upon further reduction with hydrogen, the enzyme enters the so-called Ni−C state, which is EPR active. Early ENDOR experiments on the Ni−C state showed the presence of a hyperfine coupling of a proton that was exchangeable in ^2H_2O.[14,15] Theoretical calculations on models of the Ni−C state predict a hydride bound to the [NiFe] active site;[16−18] however, the exact location and charge of the hydride remained a matter of debate. Recently, the proposal of a hydride bridge between the nickel and the iron was strongly supported by single-crystal EPR studies and density functional calculations of the Ni−C state in *D. vulgaris* Miyazaki F.[11] Direct experimental evidence for the presence of a hydrogen bound to the active site of Ni−C is still missing so far. The methods of choice to directly detect hydrogen nuclei in highly complex paramagnetic systems are electron nuclear double resonance (ENDOR) and electron spin−echo envelope modulation (ESEEM)[19,20] spectroscopy. However, the application of these methods to the Ni−C state is hindered by the fact that under reducing conditions the [4Fe4S] cluster proximal to the [NiFe] center is reduced as well, and spin−spin coupling between the two centers occurs at low temperatures.[21] This coupling affects the EPR spectrum and the relaxation behavior and thus makes the application and interpretation of advanced EPR experiments very difficult.

In the present study, we took advantage of the spectroscopic properties of the regulatory H_2-sensing [NiFe] hydrogenase (RH) from the β-proteobacterium *Ralstonia eutropha*. This protein functions as an H_2-sensor in a multicomponent signal transduction chain that controls hydrogenase gene expression in this organism on the transcriptional level.[22] Despite its regulatory role which is quite distinct from the energy-converting function of hydrogenases in strains of *Desulfovibrio*, based on sequence homology and similar EPR spectra,[23] the RH is believed to share an active site [NiFe(CO)$(CN)_2$] similar to that of standard [NiFe] hydrogenases. Reduction of the RH with hydrogen yields the Ni−C state whose EPR and FTIR spectra are almost identical to those of Ni−C in the standard hydrogenases.[23−25]

Unlike standard [NiFe] hydrogenases, however, the iron sulfur clusters of the RH remain in the oxidized state under these conditions.[24,25] This property makes the RH an ideal candidate for EPR spectroscopic investigations of the Ni−C state at low temperatures. We therefore performed ENDOR and ESEEM spectroscopy on this state with samples of purified RH. The resulting data revealed that only one exchangeable hydrogen is present in the active site of the RH in the Ni−C state. It is bound in the bridge between the nickel atom and the iron atom as a formal hydride. Upon illumination of the RH, the Ni−C state is converted into a mixture of Ni−L states, as is the case for the standard hydrogenases.[26,21] We recorded ESEEM spectra of the Ni−L1 state (for nomenclature of the Ni−L states, see ref 21) of the RH, which appears as a transient state, and no longer observed the hydride-derived signals pointing to a light-induced cleavage of the metal−hydrogen bond.

Materials and Methods

Sample Preparation. The RH was isolated from the overexpression strain *R. eutropha* HF371(pGE378), which produces the RH in 40-fold yield as compared to the wild type.[27] Large-scale cultivation, cell disruption, and protein purification were carried out as previously described.[25] As a final step, the purified preparations were dialyzed against 10 mM Tris-HCl buffer pH 8.0 and concentrated by ultrafiltration (Centriprep-10; Millipore). Cells (95 g, wet weight) yielded 3.7 mg of purified RH with a specific H_2-methylene blue oxidoreductase activity of 0.44 units/mg of protein. For solvent exchange (H_2O to ^2H_2O), the sample was diluted 5-fold with 10 mM Tris-HCl in ^2H_2O

(8) de Lacey, A. L.; Hatchikian, E. C.; Volbeda, A.; Frey, M.; Fontecilla-Camps, J. C.; Fernandez, V. M. *J. Am. Chem. Soc.* **1997**, *119*, 7181−7189.
(9) de Lacey, A. L.; Fernandez, V. M.; Rousset, M.; Cavazza, C.; Hatchikian, E. C. *J. Biol. Inorg. Chem.* **2003**, *8*, 129−134.
(10) Carepo, M.; Tierney, D. L.; Brondino, C. D.; Yang, T. C.; Pamplona, A.; Telser, J.; Moura, I.; Moura, J. J. G.; Hoffman, B. M. *J. Am. Chem. Soc.* **2002**, *124*, 281−286.
(11) Foerster, S.; Stein, M.; Brecht, M.; Ogata, H.; Higuchi, Y.; Lubitz, W. *J. Am. Chem. Soc.* **2003**, *125*, 83−93.
(12) Surerus, K. K.; Chen, M.; van der Zwaan, W.; Rusnak, F. M.; Kolk, M.; Duin, E. C.; Albracht S. P. J.; Münck, E. *Biochemistry* **1994**, *33*, 4980−4993.
(13) Albracht, S. P. J. *Biochim. Biophys. Acta* **1994**, *1188*, 167−204.
(14) Whitehead, J. P.; Gurbiel, R. J.; Bagyinka, C.; Hoffman, B. M.; Maroney, M. J. *J. Am. Chem. Soc.* **1993**, *115*, 5629−2635.
(15) Fan, Ch.; Teixeira, M.; Moura, J. J. G.; Moura, I.; Huynh, B. H.; Le Gall, J.; Peck, H. D.; Hoffman, B. M. *J. Am. Chem. Soc.* **1991**, *113*, 20−24.
(16) Pavlov, M.; Siegbahn, P. E. M.; Blomberg, M. R. A.; Crabtree, R. H. *J. Am. Chem. Soc.* **1998**, *120*, 548−555.
(17) Niu, S.; Thomson, L. M.; Hall, M. B. *J. Am. Chem. Soc.* **1999**, *121*, 4000−4007.
(18) Stein, M.; van Lenthe, E.; Baerends, E. J.; Lubitz, W. *J. Am. Chem. Soc.* **2001**, *123*, 5839−5840.
(19) Dikanov, S. A.; Tsvetkov, Y. D. *Electron Spin Echo Envelope Modulation (ESEEM) Spectroscopy*; CRC Press: Boca Raton, FL, 1992; pp 11−28.
(20) Schweiger, A.; Jeschke, G. *Principles of Pulse Electron Paramagnetic Resonance*; Oxford University Press: Oxford, 2001.
(21) Dole, F.; Medina, M.; More, C.; Cammack, R.; Bertrand, P.; Guigliarelli, B. *Biochemistry* **1996**, *35*, 16399−16406.
(22) Lenz, O.; Friedrich, B. *Proc. Natl. Acad. Sci. U.S.A.* **1998**, *95*, 12474−12479.
(23) Buhrke, T.; Brecht, M.; Lubitz, W.; Friedrich, B. *J. Biol. Inorg. Chem.* **2002**, *7*, 897−908.
(24) Pierik, A. J.; Schmelz, M.; Lenz, O.; Friedrich, B.; Albracht, S. P. J. *FEBS Lett.* **1998**, *438*, 231−235.
(25) Bernhard, M.; Buhrke, T.; Bleijlevens, B.; De Lacey, A. L.; Fernandez, V. M.; Albracht, S. P. J.; Friedrich, B. *J. Biol. Chem.* **2001**, *276*, 15592−15597.
(26) van der Zwaan, J. W.; Coremans, J. M. C.; Bouvens, E. C.; Albracht, S. P. J. *Biochim. Biophys. Acta* **1990**, *1041*, 101−110.
(27) Kleihues, L.; Lenz, O.; Bernhard, M.; Buhrke, T.; Friedrich, B. *J. Bacteriol.* **2000**, *182*, 2716−2724.

Scheme 1. Schematic Representation of Pulse Sequences Used in the Experiments[a]

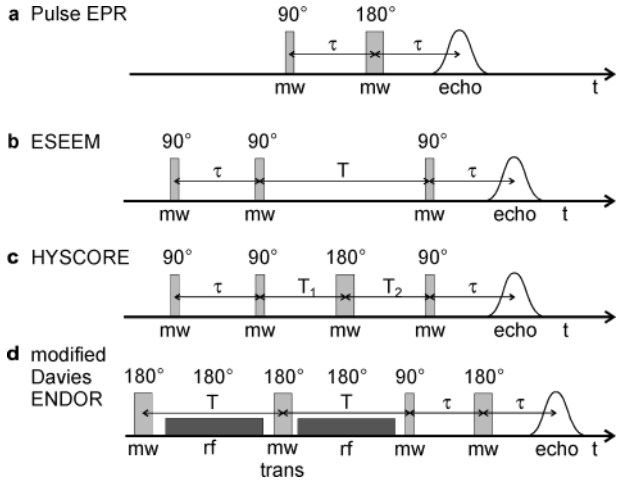

[a] (a) Field-swept echo (FSE) detected EPR; (b) three-pulse stimulated echo ESEEM; (c) four-pulse (two-dimensional) ESEEM (HYSCORE); and (d) modified Davies ENDOR with optimized polarization transfer. For details of methods, see ref 20.

(pH 8.0). Thereafter, the sample was concentrated by ultrafiltration (Microcon-10; Millipore) to the starting volume. The cycle was repeated 4 times to obtain a final concentration of >99% ^2H_2O. The protein solution was transferred to an EPR tube (Wilmad clear fused quartz 714-PQ-8) and subjected to activation with 100% $^2H_2$ for 30 min at 20 °C. The control sample that was not equilibrated in ^2H_2O was activated with 100% H_2. Finally, the samples were rapidly frozen in liquid nitrogen.

The Ni−L1 state was induced after illumination for 20 min with white light at 77 K. If the sample is annealed at 200 K for several minutes, a second Ni−L state, called Ni−L2, can be observed. After the sample is held for 1 h at 200 K, the Ni−C signal is restored.

EPR, ENDOR, and HYSCORE Experiments. All pulse EPR, orientationally selected ENDOR and ESEEM/HYSCORE (hyperfine sublevel correlation spectroscopy) measurements were carried out on a Bruker ESP 380 E FT-EPR spectrometer equipped with a dielectric ring resonator (ESP 380-1052 DL Q-H). The EPR and HYSCORE experiments were performed at $T = 5$ K, and the ENDOR experiments, at $T = 10$ K at a microwave frequency of 9.72 GHz. For EPR microwave pulses of 80 ns length, the time between the pulses was 800 ns and the repetition frequency 100 Hz. An overview of the specific pulse sequences used in the various experiments is given in Scheme 1.

Pulse ENDOR spectra of hydrogenase (in H_2O and ^2H_2O) were recorded using orientation selection in the EPR spectrum[28,29] with a modified Davies ENDOR sequence (see Scheme 1) $\pi_{mw} - \pi_{rf} - \pi_{mw,trans} - \pi_{rf} - (\pi/2)_{mw} - \pi_{mw}$ with $\pi_{mw} = 96$ ns, $\pi_{mw,trans} = 16$ ns, and $\pi_{rf} = 8\ \mu$s.[30] The modified pulse sequence has the advantage over the standard Davies ENDOR[20] that a larger ENDOR effect is obtained. The repetition frequency was chosen to be about 75 Hz, which is a compromise between the time needed for the measurement and the single-shot signal-to-noise ratio. The total measurement time for a single orientation selected ENDOR spectrum was dependent on the EPR field position, ranging from 4 h for central field positions (close to g_y) to 20 h at the edges of the EPR spectrum (near g_x and g_z); see Figure 2. During this long measurement, the frequency and phase are stable.

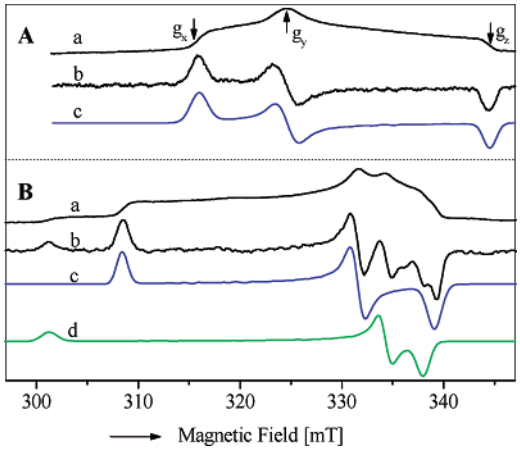

Figure 2. (A) Two-pulse field-swept echo (FSE) detected EPR spectra of the Ni−C state of the regulatory hydrogenase from *Ralstonia eutropha* (a), the first derivative using a pseudo modulation of 1 mT (b), and the simulation (blue line)(c). (B) Two-pulse FSE detected EPR spectra of the Ni−L1 and Ni−L2 states (a), the first derivative (b), and the simulations (blue line for Ni−L1 (c), green line for Ni−L2 (d)). The parameters used for the simulation are given in Table 1.

Hyperfine sublevel correlation spectroscopy[31] ($(\pi/2) - \tau - (\pi/2) - T_1 - \pi - T_2 - (\pi/2)$) modulation patterns were measured at those magnetic field positions, which correspond to the principal values of the *g*-tensor. HYSCORE is a four-pulse ESEEM technique where a series of microwave pulses is applied to the system and the times T_1 and T_2 between the pulses are scanned (see Scheme 1). In addition to the decay of the echo, which results from relaxation processes, modulations may be present from nuclei with a nuclear spin larger than zero. The frequencies of the modulations are identical to those observed in the ENDOR spectra, but the ESEEM and HYSCORE techniques have the advantage over ENDOR that additional information concerning the hyperfine interaction can be retrieved from the amplitudes. In HYSCORE, after Fourier transformation, off-diagonal peaks are observed which correlate two frequencies of the same nucleus, similar to two-dimensional NMR spectroscopy. A cross-peak correlates a nuclear transition frequency of one M_S sublevel to a nuclear transition frequency of the *same* nucleus but of the *other* M_S sublevel. It is important to note that correlations between transitions of different nuclei coupled to the same paramagnetic center are much lower in intensity. From simulations of the HYSCORE spectra with orientation selection in the EPR, information about the full hyperfine tensors of the various magnetic nuclei can be elucidated even for disordered samples.

Analytical expressions for the modulation amplitudes of ESEEM and HYSCORE have been derived elsewhere.[31,19] In total, 256 × 256 data points were acquired for T_1 and T_2, and both time increments were chosen to be either 16 or 24 ns. The repetition frequency was 100 Hz, and a four-step phase cycle was used.[32] Two sets of spectra were recorded, one at a τ value of 112 ns, the other at 200 ns. The modulation patterns were baseline-corrected and multiplied with a Hamming window function. Zero filling was performed up to 512 × 512 points, and the array was subsequently Fourier transformed into a frequency domain to obtain magnitude contour spectra.

Simulations of Spectra. Simulations of the EPR spectra were performed with the program ELSI.[33] The ENDOR spectra have been simulated with a program developed for ESEEM simulations[34] that was adapted to incorporate the ENDOR intensities. This program performs a full diagonalization of the nuclear spin Hamiltonian (vide infra) to

(28) Hoffman, B. M.; DeRose, V. J.; Doan, P. E.; Gurbiel, R. J.; Houseman, A. L. P.; Telser, J. In *Biological Magnetic Resonance, Volume 13: EMR of Paramagnetic Molecules*; Berliner, L. J., Reuben, J., Eds.; 1993; pp 151−218.
(29) Hüttermann, J. In *Biological Magnetic Resonance, Volume 13: EMR of Paramagnetic Molecules*; Berliner, L. J., Reuben, J., Eds.; 1993; pp 219−252.
(30) Schweiger, A. *Angew. Chem., Int. Ed. Engl.* **1991**, *30*, 265−292.
(31) Shane, J. J.; Höfer, P.; Reijerse, E. J.; de Boer, E. *J. Magn. Reson.* **1992**, *99*, 596−604.
(32) Gemperle, C.; Aebli, G.; Schweiger, A.; Ernst, R. R. *J. Magn. Reson.* **1990**, *88*, 241−256.
(33) Fahnenschmidt, M., Ph.D. Thesis, Technische Universität Berlin, 2000.
(34) van Gastel, M.; Coremans, J. W. A.; Jeuken, L. J. C.; Canters, G. W.; Groenen, E. J. J. *J. Phys. Chem. A* **1998**, *102*, 4462−4470.

obtain the ENDOR frequencies and intensities. It calculates the ENDOR spectrum for a fixed magnetic field setting and microwave frequency. From all possible orientations of the molecules in the frozen solution, only those are selected for which the effective *g*-value is such that the resonance condition is fulfilled. The resonance condition is fulfilled when the effective *g*-value (g_{eff}) of the molecule and the *g*-value (g_{res}) determined by the fixed magnetic field setting and microwave frequency are within the intrinsic line width of the molecule. We assume that the line width tensor, mostly determined by *g*-strain,[35] is collinear with the *g*-tensor. Principal values w_i of the line width tensor are read from the EPR spectrum and used in the simulation procedure. Then the molecule is assigned a weight that describes its contribution to the ENDOR spectrum, determined by $g_{eff} - g_{res}$ and the effective line width. Subsequently, the matrix which represents the nuclear spin Hamiltonian is computed and diagonalized, from that the ENDOR frequencies and amplitudes can be calculated. The nuclear spin Hamiltonian is given by

$$H_n = -g_n\beta_n\mathbf{B}_0 \cdot \mathbf{I} + \langle \mathbf{S} \rangle \cdot \mathbf{A} \cdot \mathbf{I} \quad (1)$$

where g_n is the nuclear *g*-value, β_n, the nuclear magneton, $\mathbf{B}_0$, the external magnetic field, $\langle \mathbf{S} \rangle$, the expectation value of the electron spin operator, and $\mathbf{A}$, the hyperfine tensor. For a nucleus with spin $^1/_2$, six parameters are required to specify the hyperfine tensor. Each transition was assigned a line width of 280 kHz. When all possible orientations have been considered (the orientational averaging includes typically 10 000 orientations), the array can be compared directly with the experimental spectrum.

Simulations of the ^{2}H HYSCORE spectra were also performed with the program for simulating ESEEM spectra, described in ref 34. The program has been extended to incorporate the modulation formula for HYSCORE[31] and to store the modulation amplitudes in a two-dimensional instead of a one-dimensional array. The program calculates the HYSCORE spectrum at a fixed magnetic field setting and microwave frequency in exactly the same way as in the simulation of an ENDOR spectrum, with the exception that the HYSCORE amplitudes are calculated from the eigenvectors of the nuclear spin Hamiltonian. Nuclear quadrupole interaction of the ^{2}H nucleus was neglected since it is rather small (see Discussion). The amplitudes are stored in a two-dimensional array in the frequency domain and are assigned a line width of 120 kHz (which is a reasonable value for the line width excluding quadrupole broadening). Again, after all orientations are considered, the array can be compared directly with the experimental spectrum.

Results

EPR. The field-swept echo (FSE) detected EPR spectra of the Ni−C state of *R. eutropha* hydrogenase are shown in Figure 2A(a). The spectrum is characterized by a rhombic *g*-tensor with two larger *g*-values of 2.197 and 2.139 and one smaller *g*-value of 2.015. The first derivative is also shown in spectrum b together with the corresponding simulation (c). The *g*-values and line width parameters used in the simulation are summarized in Table 1. The *g*-values are close to those observed for the Ni−C state of the standard hydrogenase of *D. vulgaris* Miyazaki F (Table 1). This indicates that the Ni−C states of these enzymes are very similar with respect to their basic electronic structure.[25] In the regulatory hydrogenase, no signal arising from either of the [FeS] centers is observed at low temperatures (not shown).

After illumination with white light at 77 K, new EPR signals appear, which correspond to another redox state. This state has also been observed in standard hydrogenases and is denoted Ni−L1[21] (see Figure 2B). If the sample is annealed at 200 K for several minutes, a second Ni−L state can be observed, denoted Ni−L2, which is significantly different from the original Ni−L1 state. A superposition of both states is shown in Figure 2B(a,b), and the respective simulations of Ni−L1 and Ni−L2 spectra are shown in c and d. The *g*-values and line width parameters for both states are included in Table 1. The principal *g*-tensor components of the two Ni−L states are very different, and the line widths are somewhat smaller than those found for Ni−C. Noteworthy are the increased g_z values of the light-induced states that clearly deviate from $g_e \approx 2.00$.

Table 1. The Principal *g*-Tensor Values and Line Width Parameters (w_i) [mT] Obtained from the Simulation of the EPR Spectra of the Ni−C, Ni−L1, and Ni−L2 States of the Regulatory Hydrogenase of *Ralstonia eutropha* in H_2O Activated with H_2

	R. eutropha						*D. vulgaris*	
	Ni–C[a]		Ni–L1[b]		Ni–L2[b]		Ni–C[c]	Ni–L2[c]
	g	w_i	*g*	w_i	*g*	w_i	*g*	*g*
x	2.197	1.6	2.251	1.0	2.305	1.5	2.198	2.298
y	2.139	1.6	2.094	1.1	2.077	1.0	2.142	2.116
z	2.015	1.1	2.046	1.1	2.054	1.2	2.012	2.045

[a] From ref 23. [b] This work. [c] From ref 11.

ENDOR. The absence of the spin−spin coupling between the proximal [4Fe−4S] cluster and the [NiFe] center enabled us to investigate the surrounding of the active center with hyperfine-resolving techniques. We recorded orientationally selected pulse ^{1}H ENDOR[28,29] spectra at 26 different field positions over the EPR envelope. The technique has been applied earlier to related systems.[36,37] To identify exchangeable protons in the spectra, we also obtained pulse ^{1}H ENDOR spectra of the RH in ^2H_2O activated with $^2H_2$ gas. A selection of the spectra (in H_2O activated with H_2) is shown in Figure 3.

The spectra show a rich structure of bands. Each proton is expected to give rise to two lines whose frequencies are symmetrically displayed around the ^{1}H Larmor frequency $\nu_{^1H}$. We will concentrate on the high-frequency part of the spectrum, that is, $\nu_{ENDOR} > \nu_{^1H}$. At the high field edge (343.0 mT), molecules are selected that are oriented such that their g_z-axis is parallel to the magnetic field, and strongly shifted ENDOR lines at 17.7, 20.7, and 23.7 MHz are observed.[38] At lower magnetic fields, molecules with so-called noncanonical orientations are resonant, and all three bands split into two. For example, the band at 23.7 MHz splits, and two signals at 22.6 and 24.2 MHz appear in the spectrum recorded at 336.0 mT. The two split signals join again in the spectrum recorded near the low field edge ($\sim g_x$) at 316.5 mT, where one band is observed at 21.8 MHz. The band at 20.7 MHz in the spectrum of 343.0 mT follows a similar pattern and appears at 18.8 MHz in the spectrum of 316.5 mT. The signal at 17.7 MHz seems to vary more strongly with magnetic field, indicating a larger anisotropic hyperfine interaction, but can unfortunately not be followed over the complete magnetic field range.

In Figure 4, ENDOR spectra recorded near g_z at 343.0 mT are shown, one for Ni−C in H_2O activated with H_2, one in ^2H_2O activated with $^2H_2$. The bands at about 17.7, 20.7, and 23.7 MHz are still present after exchange of the solvent with ^2H_2O, albeit

(35) Hagen, W. R. *J. Magn. Reson.* **1981**, *44*, 447−469.
(36) Gessner, Ch.; Stein, M.; Albracht, S. P. J.; Lubitz, W. *J. Biol. Inorg. Chem.* **1999**, *4*, 379−389.
(37) Müller, A.; Tscherny, I.; Kappl, R.; Hatchikian, E. C.; Hüttermann, J.; Cammack, R. *J. Biol. Inorg. Chem.* **2002**, *7*, 177−194.
(38) Note that orientation selection is not perfect and leads to a slight splitting also at this field value.

Table 2. Isotropic and Dipolar Proton Hyperfine Coupling Constants [MHz] and Direction Cosines of the Principal Axes of the Hyperfine Tensors for H1, H2, and H3 of Ni−C in RH of *R. eutropha*

	hyperfine couplings[b]								direction cosines		
position	a_{iso}	A'_x	A'_y	A'_z	A_x	A_y	A_z	axes	l_x	l_y	l_z
H1	17.6	2.9	−1.0	−1.8	20.5	16.6	15.8	*a*	0.506	−0.021	0.862
								b	0.147	−0.983	−0.111
								c	0.850	0.183	−0.494
H2	12.8	3.7	−1.6	−2.2	16.5	11.2	10.6	*a*	0.557	−0.333	0.760
								b	−0.223	−0.942	−0.243
								c	0.798	−0.041	−0.602
H3[c]	−3.5	21.9	−7.3	−14.5	18.4	−10.8	−18.0	*a*	−0.63	0.54	−0.55
								b	0.21	0.81	0.55
								c	0.74	0.23	−0.63

[a] The quantities A'_i ($i = x, y, z$) and a_{iso} correspond to the dipolar values and the isotropic value of the tensor; $A'_i = A_i - a_{iso}$. The direction cosines l_i are given in the crystal axes system (*abc*), for which the crystal structure of the standard hydrogenase from *D. vulgaris* Miyazaki F was used.[3] [b] For errors, see text. [c] The sign of the principal values has been chosen to agree with those found in DFT calculations (see text and ref 42).

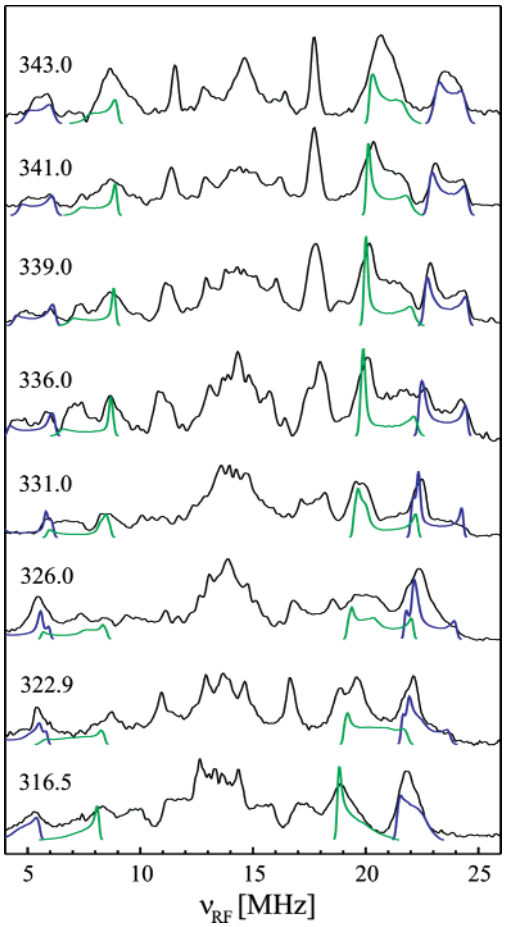

Figure 3. Orientation-selected pulse ENDOR spectra of Ni−C of the RH in H_2O, activated with H_2 gas. The field positions (mT) at which the spectra were recorded are included in the figure. Also included in the figure are the simulations for the protons H1 (blue line, strongest coupling) and H2 (green line). Simulation parameters are included in Table 2 and the Materials and Methods section.

with slightly changed intensities: they belong to nonexchangeable protons. The shape of the two bands and their field dependence are similar over the whole field range. A direct interpretation of the differences in intensity is impeded, however, by a solvent dependent relaxation behavior, which influences the line width. This has also been observed in other hydrogenases.[14,15]

Since the gyromagnetic ratio for deuterium is about 6.5 times smaller than that for hydrogen, ^{2}H ENDOR lines are expected

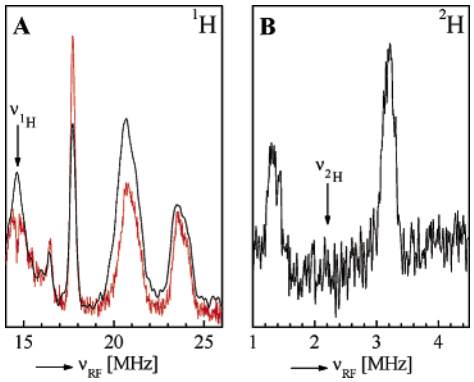

Figure 4. ^{1}H and ^{2}H ENDOR spectra of the Ni−C state of the RH. (A) RH in H_2O activated with H_2 (black) and in ^2H_2O activated with $^2H_2$ (red) in the ^{1}H ENDOR region; (B) RH in ^2H_2O activated with $^2H_2$ in the ^{2}H ENDOR region. The spectra are recorded at an EPR field position of 343.0 mT.

around ∼2.2 MHz at X-band. ^{2}H ENDOR signals have been observed in the ^2H_2O exchanged sample as shown in Figure 4B, indicating the presence of at least one exchangeable proton. In the sample in H_2O, no signals were observed in this region. Because of the inherent low sensitivity of the ENDOR technique around 2 MHz, the hyperfine anisotropy of the exchangeable proton has further been analyzed by HYSCORE spectroscopy, which has a much better sensitivity than ENDOR in this frequency range (see below).

Simulations of the nonexchangeable protons observed in the ENDOR spectra have been performed to elucidate the hyperfine coupling constants. The simulations of the ^{1}H ENDOR lines are shown in Figure 3, and the hyperfine tensors resulting from the simulations are given in Table 2. The two protons with the largest shifts in the ENDOR spectra have been simulated with hyperfine tensors H1 and H2 that are predominantly isotropic (a_{iso} of 17.6 and 12.8 MHz, respectively). Such strong isotropic couplings indicate that these protons must be close to an atom that carries a large amount of the unpaired spin density. The principal directions of the main dipolar axis (*x*) of H1 and H2 differ by 22°, and the field dependence of these two couplings are similar. This indicates that these protons are most probably attached to the same C-atom, for example, a CH_2 group of one of the cysteines. The fitting errors for these protons are estimated at ±0.5 MHz for the principal values and ±5° for the dipolar axis and ±10° for the other principal directions. The hyperfine tensor of an additional nonexchangeable proton in the spectra also exhibits a large isotropic hyperfine interaction (6−7 MHz).

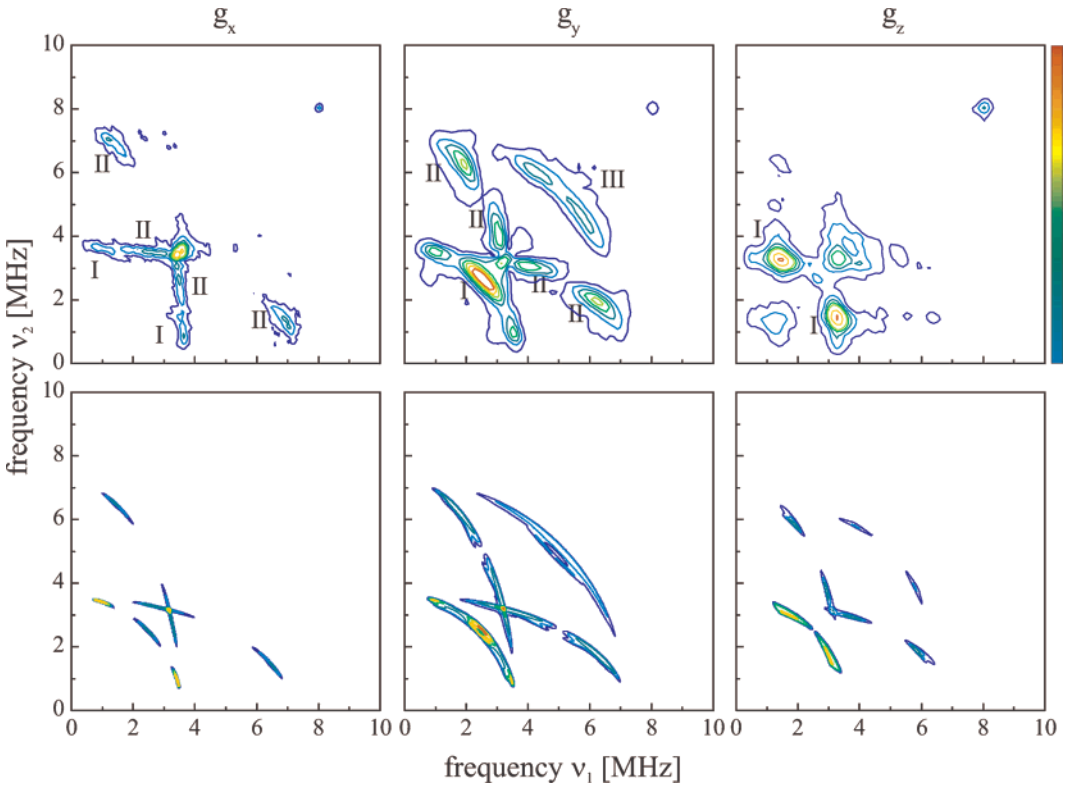

Figure 5. Experimental (top) and simulated (bottom) orientation selected HYSCORE spectra at g_x (317.0 mT), g_y (325.0 mT), and g_z (343.5 mT) of the Ni−C state of the RH in ^2H_2O activated with $^2H_2$. The ^1H hyperfine parameters used in the simulations are given in Table 2 and have been scaled down by a factor of $\gamma(^1H)/\gamma(^2H) = 6.514$ to account for the different gyromagnetic ratios of ^1H and ^2H. The different cross-peaks are labeled with I, II, and III (see text).

But this coupling is not sufficiently resolved to perform a reliable simulation; no parameters for this proton are included in Table 2.

HYSCORE. In the hydrogenase sample in H_2O, we observed modulations of proton nuclei in HYSCORE at the ^1H Larmor frequency (about 14 MHz) and two weak signals, which hardly exceed the noise level on the diagonal at 2.2 and 3.4 MHz (not shown). For the deuterated sample, we observe, however, strong modulations around the ^2H Larmor frequency (about 2 MHz) that span from 0 to 8 MHz. This shows that at least one proton in the surrounding of the spin carrying [NiFe] center is exchangeable with ^2H and gives rise to strong signals in this range. Three HYSCORE spectra for the Ni−C state of *R. eutropha* hydrogenase in ^2H_2O, recorded at the magnetic field settings that correspond to the principal values of the *g*-tensor, are depicted in Figure 5. The spectra show several diagonal peaks and off-diagonal cross-peaks in the region between (0, 0) and (8, 8) MHz. The peaks on the diagonal stem from incomplete population inversion; that is, some of the molecules have not "seen" the π pulse and give rise to modulations that contribute to the peaks on the diagonal like in a three-pulse ESEEM experiment. We will therefore concentrate on the cross-peaks.

At high magnetic field (g_z) two strong cross-peaks (labeled I) are observed at (1.4, 3.2) MHz and (3.2, 1.4) MHz. When going to an intermediate field (g_y), the strong cross-peaks (I) smear out and form a curve with intensity maxima at (1.0, 3.4) MHz, (2.6, 2.6) MHz, and (3.4, 1.0) MHz. Additional cross-peaks, all labeled II, are observed at (3.0, 4.0) MHz and (4.0, 3.0) MHz and at (1.8, 6.0) MHz and (6.0, 1.8) MHz. Between (4.0, 6.0) MHz and (6.0, 4.0) MHz, a curve of low intensity (III) is observed. This curve occurs at double the frequencies of curve I. Going to a lower magnetic field (g_x), curve I has become so weak that only two low-intensity cross-peaks at (0.8, 3.5) MHz and (3.5, 0.8) MHz remain visible. The two cross-peaks at (3.0, 4.0) and (4.0, 3.0) MHz now have an almost horizontal/vertical intensity distribution, which is centered at (2.7, 3.5) MHz and (3.5, 2.7) MHz. The cross-peaks at (1.8, 6.0) MHz and (6.0, 1.8) MHz have shifted to (1.4, 6.4) MHz and (6.4, 1.4) MHz. Curve III is no longer observed.

The signals that exchange in ^2H_2O and that are observed in the ^2H HYSCORE spectra have all been simulated with one hyperfine tensor (H3). In the simulations (Figure 5, lower part), the line width parameters w_i ($i = x, y, z$) as given in Table 1 have been used. For the HYSCORE spectra, the simulations reproduce all essential features (except the line width, cf. Discussion). This shows that only one exchangeable proton can be analyzed with reliability. The curve labeled I corresponds to correlations between the single-quantum transitions of the two M_S manifolds, curve II, between a single-quantum frequency of one M_S manifold and the double-quantum frequency of the other M_S manifold, and curve III, between the double-quantum frequencies of both M_S manifolds. Because of the abundant information present in the HYSCORE spectra, the fitting error of this tensor is relatively small (about 0.2 MHz for the principal values and 10° for the principal directions). The nuclear quadrupole splitting of the deuterium nucleus is typically in the range of $e^2qQ/h = 200$ kHz.[39] However, for bridging metal hydrides (M−^{2}H−M), much smaller values (~20 kHz) from

(39) Lucken, E. A. C. *Nuclear Quadrupole Coupling Constants*; Academic Press: London, 1969.

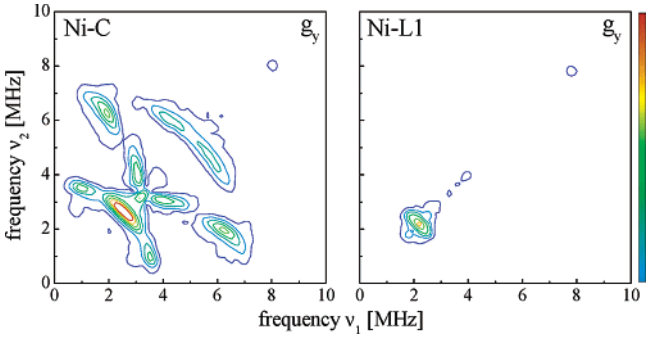

Figure 6. HYSCORE spectra measured at g_y (325.0 mT) for the Ni−C and Ni−L1 states. The ^{2}H Larmor frequency is 2.1 MHz. Note the disappearance of the larger resonances (peaks) in the Ni−L1 spectrum.

solid-state deuterium NMR spectroscopy and ab initio quantum chemistry have been reported.[40,41] For hydrogenase, the bonding interaction to both the nickel and the iron probably reduces this value as compared to that for a singly bonded deuterium. This value is smaller than the line width observed in the HYSCORE spectra. Test simulations have been performed which included a quadrupole coupling of 200 kHz. This led to only a small increase in the line width. Therefore, to keep the number of fit parameters minimal, the quadrupole interaction has been neglected in the simulations.

After illumination of the Ni−C state at 77 K for 20 min, a full conversion to the Ni−L1 state is reached. We recorded HYSCORE spectra for the Ni−L1 state of RH in ^2H_2O activated with $^2H_2$. A comparison of the HYSCORE spectra in the ^{2}H range for the Ni−C and Ni−L1 states recorded at one field position (g_y) is shown in Figure 6. The signals from the strongly coupled exchangeable proton are lost in Ni−L1. The other orientations show a very similar effect. After warming of the sample for about 1 h at 200 K, and cooling again to 5 K, the Ni−C signal is completely restored, and the strong bands assigned to the exchangeable proton in the HYSCORE spectra reappear.

Discussion

The regulatory hydrogenase is characterized by nearly the same *g*-tensor principal values as the standard hydrogenases (cf. Table 1). Because of the high sequence homology to the standard hydrogenases and the similarity of the EPR and FTIR spectra, we assume that the electronic and geometric structure of the Ni−C state of the RH, including the orientation of the *g*-tensor,[11] is similar to that of the standard hydrogenases. In the Ni−C state of these enzymes, the Ni is in the Ni(III) state and the unpaired electron occupies predominantly a d_{z^2} orbital as also found in the oxidized states (Ni−A, Ni−B).[11] In the Discussion, we will first address details of the simulations, then focus on assigning the hyperfine tensors H1, H2, and H3 to protons in the vicinity of the nickel atom, and finally discuss the light sensitivity of the Ni−C state.

Simulations of Spectra. Simulations of the ENDOR spectra have been performed to elucidate the hyperfine tensors H1 and H2 of two nonexchangeable protons. From simulations of the HYSCORE spectra, the hyperfine tensor H3 of an exchangeable proton has been obtained. The simulations of the ^{1}H ENDOR and ^{2}H HYSCORE spectra are included in Figures 3 and 5, respectively. The simulations adequately describe the experimental spectra.

The ENDOR simulations for the nonexchangeable protons are able to reproduce the frequencies of the bands in the experimental spectrum and also, partially, the shape of the bands. For the latter, however, the agreement is not perfect. The reason for this is that the simulations take *g*-strain effects into account only in a rudimentary manner. To consider such *g*-strain effects, the line width observed in the EPR spectrum (cf. Table 1) is used to estimate the contribution of a molecule with a particular orientation with respect to the magnetic field. This contribution is determined by the difference of the effective *g*-value of this molecule and the *g*-value given by the fixed microwave frequency and magnetic field according to the resonance condition, divided by the EPR line width. The line width in the simulation of the ENDOR spectrum is chosen to be isotropic (280 kHz), and to keep the parameter set for the simulation to a minimum, other mechanisms that contribute to the line width (e.g., hyperfine strain or frequency-dependent relaxation times) are not included. The line width assigned to the bands in the HYSCORE simulations of the ^{2}H region is also isotropic (120 kHz). Moreover, in this case, the nuclear quadrupole splitting is neglected. Since the nuclear quadrupole interaction of ^{2}H was not resolved in the experimental spectra, it must be assumed that the coupling is indeed small ($\leq$120 kHz). Even though the simulation of the line width has been simplified in order to keep the number of parameters limited, experiment and simulation are in good agreement.

Assignment of the Hyperfine Tensors of the Nonexchangeable Protons. Recently, the full *g*-tensor of the standard hydrogenase from *D. vulgaris* Miyazaki F was determined by single-crystal EPR experiments and supported by DFT calculations.[11] Since this hydrogenase is very similar to the regulatory hydrogenase of *R. eutropha* with respect to all spectroscopic characteristics,[24,25] we assume that the *g*-tensor orientation found for the standard hydrogenase is retained in the regulatory hydrogenase. This structural information allows us to determine the location of the exchangeable proton and the nonexchangeable protons in the RH.

The only nonexchangeable protons that are sufficiently close to the large spin density at the [NiFe] center to be compatible with an isotropic coupling of about 18 and 13 MHz are the β-CH_2 protons of the cysteines. Comparison of the directions of the dipolar axes with the direction of the vector joining the β-CH_2 protons and the Ni-atom, which carries the major part of the spin density, yielded minimal angles of 15° for both β-CH_2 protons of cysteine 482 of the large subunit of RH (HoxC[27]). This residue corresponds to cysteine 549, in the large subunit of *D. vulgaris* hydrogenase (HydB). We therefore assign the signals of the nonexchangeable protons to the β-CH_2 protons of this cysteine. This is the cysteine that for *D. vulgaris* hydrogenase is in the direction of the d_{z^2} orbital and thus carries a large part of spin density (see Figure 1).[11,42]

Assignment of the Hyperfine Tensor of the Exchangeable Proton. DFT calculations of the Ni−C intermediate[18] indicated that good agreement is found between experimental and calculated *g*-values when a hydride occupies the position "X" of the bridging ligand and the Ni is in a formal Ni(III) state. In

(40) Jarrett, W. L.; Farlee, R. D.; Butler, L. G. *Inorg. Chem.* **1987**, *26*, 1381−1383.
(41) Guo, K.; Jarrett, W. L.; Butler, L. G. *Inorg. Chem.* **1987**, *26*, 3001−3004.
(42) Stein, M.; Lubitz, W. *Phys. Chem. Chem. Phys.* **2001**, *3*, 5115−5120.

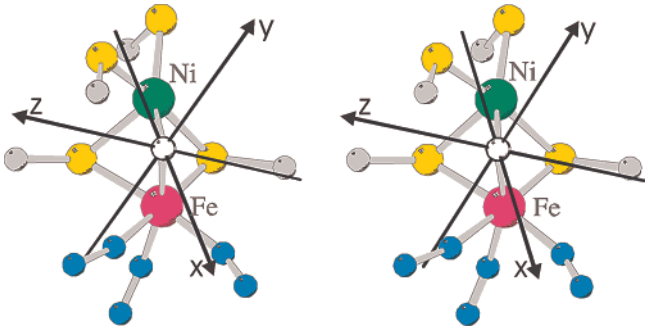

Figure 7. Stereoview showing the directions of the principal axes of the hyperfine tensor for the exchangeable hydrogen in the active [NiFe] center. The position of the hydride has been identified with the bridging position (white); see Figure 1.

later DFT calculations,[42] also the hyperfine tensor of this hydride was calculated ($a_{iso} = -8.7$ MHz, $A' = +18.6, -7.5, -11.1$ MHz). These numbers can be compared with the experimental ones found for the exchangeable proton in this work. The hyperfine tensor H3 for the exchangeable proton obtained from simulation of the HYSCORE measurements shows a fairly small isotropic hyperfine coupling as compared to the anisotropic part of the tensor. It has principal values of +21.9, −7.3, and −14.5 MHz and an isotropic value of −3.5 MHz (see Table 2). Although the agreement with the calculations is not perfect, the experimental and calculated couplings have the same magnitude. Additionally, the geometry optimization showed that the distance of the bridging hydrogen to the Ni is 1.61 Å and is 1.72 Å to the Fe. This shows that the exchangeable proton has to be in the first coordination sphere of the nickel atom. Although the simple point-dipole model has limited accuracy for distances shorter than ~2 Å,[15] a rough estimate of the distance between Ni and the hydride ion can be obtained from this model. Using the major dipolar coupling of the hydrogen $A'_x = A'_{||} = +21.9$ MHz and a spin density at the Ni of 0.6,[42] we obtain $r = 1.63$ Å[43] in astonishingly good agreement with the value of 1.61 Å obtained by geometry optimization of an Ni−C cluster model using DFT.[42]

Further evidence for such an assignment is expected from evaluation of the tensor axes. Here it is assumed that the axis of the largest positive dipolar value points approximately from the spin carrying Ni to the hydrogen. First a comparison of the directions of the principal axes of the hyperfine tensor with the *g*-tensor has been performed. This yielded an approximate alignment of the orientations of A_x and g_x (angle 13°), of A_y and g_z (angle 18°), and of A_z and g_y (angle 18°). With the knowledge of the orientation of the *g*-tensor with respect to the geometry of the [NiFe] site,[11] the hyperfine tensor axes can be placed onto the bridging ligand (see Figure 7). The *x*-axis is associated with the largest anisotropic hyperfine coupling (21.9 MHz), and this axis is almost parallel with the Ni−H bond direction. This provides further evidence that the exchangeable proton can indeed be assigned to a hydrogen (or a formal hydride) in the bridging position between nickel and iron.

It is striking that the isotropic hyperfine interaction found here (and with DFT calculations[42]) is much smaller than that expected for a hydride covalently bound to a nickel atom.[44,45] This might be caused by the fact that the hydrogen is approximately lying in the nodal plane of the spin carrying orbital $3d_{z^2}$ at the nickel. Additional effects may arise from the presence of the iron which may cause a redistribution of the actual charge/spin density in the complex.[46]

Light Sensitivity of the Ni−C State. The rich structure observed in the ^{2}H region of the HYSCORE spectra of the Ni−C state of the RH in ^2H_2O activated with $^2H_2$ is lost after illumination and conversion to the Ni−L1 state (see Figure 6). The most plausible explanation for this is that the metal−hydrogen bond is cleaved and the hydrogen leaves the bridging position "X" (see Figure 1). Earlier ENDOR experiments[14] and DFT calculations of the Ni-L state[18] have suggested that the bridging position is empty and the nickel has a formal oxidation state of +1, whereas it is +3 for Ni−C. Upon warming the sample to 200 K, we recover the Ni−C state. Thus, most probably, the cleavage involves translocation of a proton (H^+) away from the bridging position, but it remains near the [NiFe] center. It can reoccupy the bridging position when the temperature is raised to 200 K. Possible candidates for the proton acceptor are the amino acids surrounding the [NiFe] center. The most likely is either one of the terminal cysteines ligated to the nickel or the nearby arginine 411 of the so-called 4L-motif,[13] that is conserved in all hydrogenases (this is arginine 475 in *D. vulgaris* hydrogenase). Experiments are under way in our laboratories to identify this proton acceptor.

Conclusion and Outlook

We have measured ENDOR and HYSCORE spectra for the regulatory hydrogenase of *Ralstonia eutropha*. The hyperfine tensors of two nonexchangeable protons have been analyzed and assigned to the β-CH_2 protons of the cysteine 482, which carries a large part of the spin density.[11,42] In addition, one exchangeable proton is observed which has a predominantly anisotropic hyperfine tensor. Based on an analysis of the magnitudes and directions of the hyperfine tensor principal components, this hydrogen is assigned to reside in a bridging position between nickel and iron in Ni−C. The position of the hydrogen is estimated from the hyperfine tensor axis and a simple point-dipole approach and agrees reasonably well with DFT calculations on geometry optimized model clusters of the active site.[42] This DFT calculations strongly suggest the presence of a hydride (H^-) in the bridge between nickel and iron, which are formally in the Ni(III) and Fe(II) oxidation states.

Upon illumination, the hyperfine coupling associated with the exchangeable proton is lost, which indicates a dissociation of the metal−hydrogen bond in the Ni−L1 state. The dissociation which involves a proton translocation[11,14] is reversible. When the sample is warmed to about 200 K for 1 h, the Ni−C state is fully recovered, which indicates that the proton remains close to the active site. The experiments, for the first time, give direct information on the binding position of the hydride after heterolytic cleavage of dihydrogen in the active site of a regulatory hydrogenase. The proton from this process is most

(43) An estimation of the Ni−hydride distance using data from DFT calculations ($\rho_{Ni} = 0.595$, $A'_{||} = +18.6$ MHz)[42] yields $r = 1.72$ Å. The geometry optimization of the DFT model gave $r = 1.61$ Å showing that the error of the point dipole model at these distances lies in the range 0.1−0.15 Å.

(44) Morton, J. R.; Preston, K. F. *J. Chem. Phys.* **1984**, *81*, 5775−5778.
(45) Stein, M.; van Lenthe, E.; Baerends, E. J.; Lubitz, W. *J. Phys. Chem. A* **2001**, *105*, 416−425.
(46) Note that the spin density on the iron itself is very low; see: Huyet, J. E.; Carepo, M.; Pamplona, A.; Franco, R.; Moura, I.; Moura, J. J. G.; Hoffman, B. M. *J. Am. Chem. Soc.* **1997**, *119*, 9291−9292.

probably attached to a remote site in the Ni−C state or has already left the site since no coupling from a second exchangeable proton could be detected in our experiments.

Due to the great similarity of the spectroscopic data found for the Ni−C state in the regulatory and the standard hydrogenases it is expected that the binding situation of the hydrogen in the latter is basically the same. The exact nature of the metal−hydrogen bond, the actual charge of the hydride and the metal(s), the role of the Fe atom, and the identity of the proton acceptor in the Ni−L1 state are still unknown and continue to be under investigation. Furthermore, experiments to directly measure the hyperfine couplings of the hydride in standard hydrogenases, for example, of *D. vulgaris* Miyazaki F, and experiments to determine the electronic transitions associated with the conversion from Ni−C to Ni−L are in progress in our laboratory.

Acknowledgment. The authors are grateful to Stefanie Foerster and Matthias Stein (TU Berlin) for many stimulating discussions. This work was supported by the Deutsche Forschungsgemeinschaft (Sfb 498, TP C1 and C2), the Max-Planck-Gesellschaft, and the Fonds der Chemischen Industrie.

JA036624X